

Development of high performance fiber reinforced cement composites (HPFRCC) for application as a transition layer of reinforced beams

Desenvolvimento de compósitos cimentícios de elevado desempenho armados com fibras para aplicação como substrato de transição de vigas de concreto



V. J. FERRARI^a
vladimirjf@hotmail.com

A. P. ARQUEZ^b
anaeng@hotmail.com

J. B. DE HANAI^c
jbhanai@sc.usp.br

R. A. DE SOUZA^a
rsouza@uem.br

Abstract

This study presents the development and behavior analysis of high performance fiber reinforced cement composites (HPFRCC). The described materials were specifically developed for application as a transition layer: a repair layer that constitutes the stressed chord of reinforced concrete beams strengthened in flexure with carbon fiber reinforced polymers (CFRP). Nineteen different composites were produced by the hybridization process, varying the conventional short steel fiber and steel microfiber (manufactured exclusively for this research) contents to modify the microstructure of the material, thus enhancing the stress transfer process from the cement matrix to the fibers. To analyze the response to flexural loading, the composites underwent three point bending tests in notched prism specimens. The response of the material was obtained considering strength and tenacity parameters (flexural and fracture). There was evidence of high performance by the composites with a pseudo-hardening behavior.

Keywords: higher performance fiber reinforced cement composite (HPFRCC), reinforced concrete beams, transition layer, steel microfiber.

Resumo

Este estudo apresenta o desenvolvimento e a análise do comportamento de compósitos cimentícios de elevado desempenho armado com fibras. O material descrito foi especificamente desenvolvido para aplicação como um substrato de transição: uma camada de transição que forma o banzo tracionado de vigas de concreto armado reforçadas à flexão com polímeros reforçados com fibras de carbono (PRFC). Dezenove diferentes compósitos foram produzidos pelo processo de hibridização, variando o volume de fibras curtas convencionais de aço e microfibras de aço (produzidas especificamente para este estudo) para modificar a microestrutura do material numa tentativa de melhorar o processo de transferência das tensões da matriz para as fibras. Para analisar a resposta do material à flexão, os compósitos foram submetidos a ensaios de flexão em três pontos em corpos de prova prismáticos com entalhe central. A resposta do material foi obtida considerando-se parâmetros de resistência e de tenacidade (flexional e ao fraturamento). Ficou evidenciado o elevado desempenho dos compósitos com um comportamento de pseudo-encruamento.

Palavras-chave: compósitos cimentícios de elevado desempenho armados com fibras; vigas de concreto armado; substrato de transição, microfibras de aço

^a State University of Maringá, Department of Civil Engineering, Maringá, Brazil;

^b Structural Engineer, Sao Paulo, Brazil;

^c University of Sao Paulo, School of Engineering of São Carlos, Sao Carlos, Brazil.

1. Introduction

It is well known that concrete is a relatively brittle material. Randomly distributed short fibers may improve toughness of cementitious matrices by preventing or controlling the initiation, propagation or coalescence of cracks (Bentur and Mindess [1]). In this way, concrete properties may be improved in a certain level (but not in all levels) if one type of fiber is chosen as reinforcement (Yao et al. [2]). If two types of fibers are used the influence in concrete properties will be even higher.

It has been shown by using the concept of hybridization with two different types of fibers incorporated in a common cement matrix, that the hybrid composite can offer more attractive properties. It occurs because the presence of one type of fiber enables a more efficient utilization of the potential properties of the other type of fiber (Mobasher and Li [3]).

According to Ferreira et al. [4], the modifications resulting from the addition of steel fibers to concrete, at relatively low rates (a maximum of 2%), are restricted only to the post-peak stage of the load-

ing history. Under such conditions (at low rates), the steel fibers are not sufficient to inhibit the matrix cracking process which precedes the maximum load (subcritical growth of cracks).

In order to improve the cement-based composite behavior during the pre-peak stage, the effect of incorporating steel microfibers with the conventional steel fibers was studied. In this way, a modification of the microstructure of the composite occurs, improving the process of stress transference from the matrix to the fibers.

These materials were specifically developed for an application as a transition layer (Figure [1]) and nineteen different composites were prepared in two stages (Stage I and Stage II). In the Stage I, the composites were developed for application as a transition layer of reinforced concrete beams strengthened by bonding CFRP sheets. In the Stage II, the composites were developed for application in transition layers of strengthened beams by the insertion of CFRP laminates in notches executed in this layer (near-surface mounted technique).

In engineering practice (Figure [1]), the tensile bottom chord of reinforced concrete beams to be strengthened are frequently found

Figure 1 - Aspect of a tensile bottom chord of beam damaged by concreting deficiency and by reinforcement corrosion

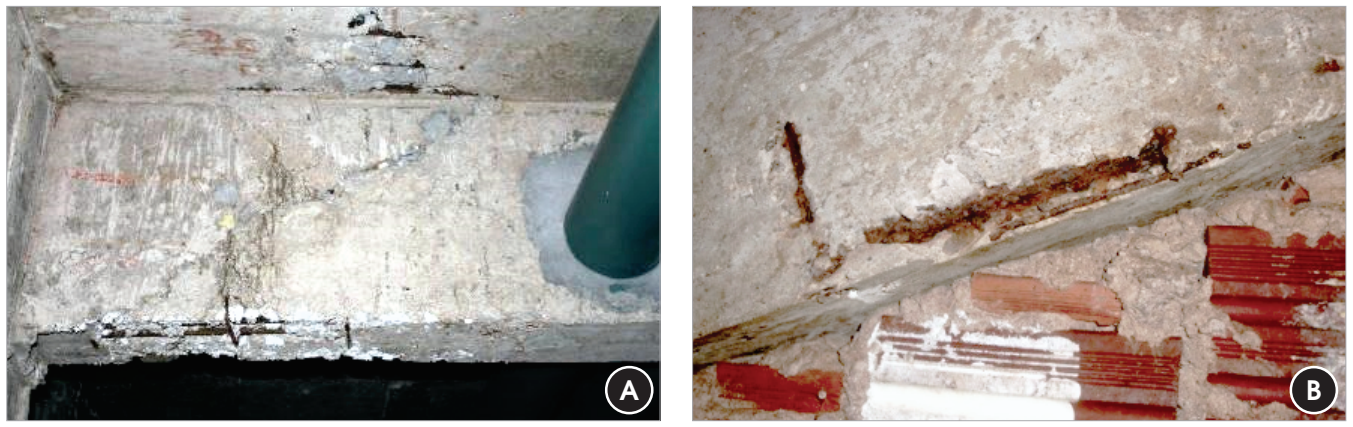


Figure 2 - Transition layer of a reinforced concrete beam strengthened with CFRP

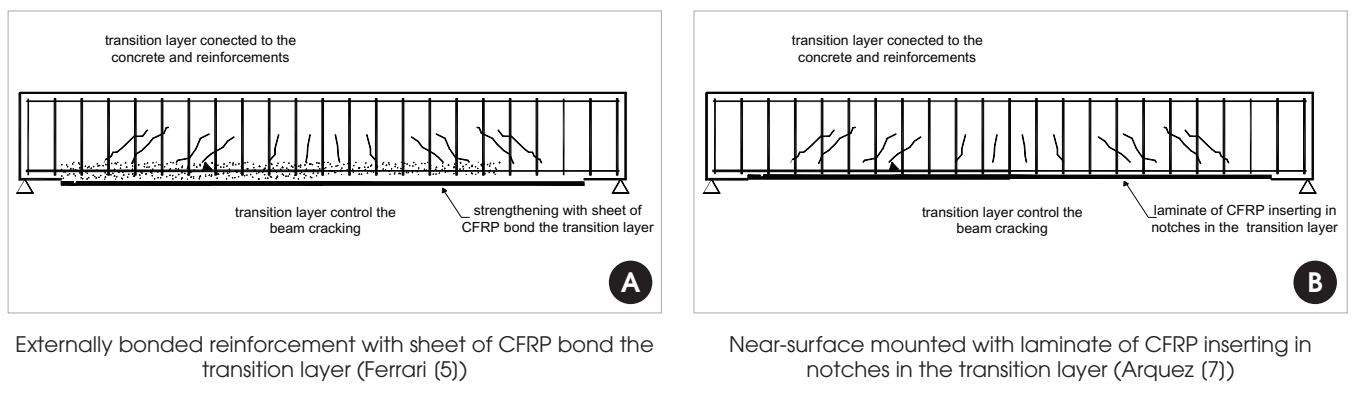
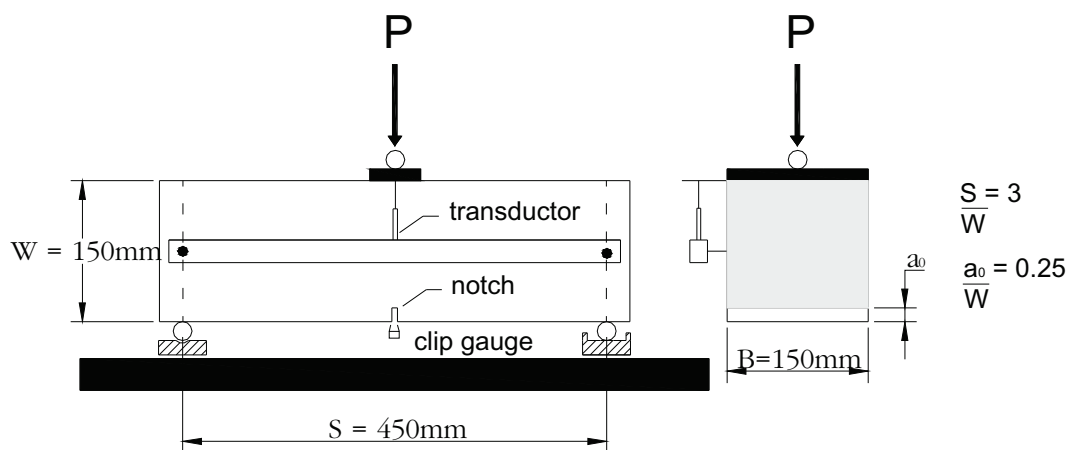


Figure 3 - Dimensions of the specimens and general test configuration



to be damaged by mechanical actions, corrosion effects or cracking. In such cases, the strengthening process must be preceded by the recovery of the bottom chords.

For this purpose, Ferrari [5] proposed the development of a high performance Portland cement-based composite with steel fibers and microfibers, destined to construct a transition layer as indicated in Figure [2a]. The main idea was to remove part of the tensile bottom chord of the beams and reconstitute them using cement composite. The concept of transition layer is to create new bottom chords composed of a cement-based material with more appropriate characteristics for bonding the polymer reinforcement.

Thus, in this study, new results were added to the results already presented in Ferrari [5]. These new results were obtained through the development and analysis of new composites using the near-surface mounted technique, i.e., by inserting carbon fiber laminates in notches prepared in the transition zone (Figure 2b).

2. High performance fiber reinforced cement composites (HPFRCC)

2.1 Test setup

In order to evaluate the tensile strength of the developed cement-based composites, three point bending tests of prismatic specimens (150 mm x 150 mm x 500 mm) with central notch as recommended by Rilem [6] has been carried out. The tests were conducted in the Laboratory of Structures of the School of Engineering of São Carlos. Figure [3] shows the general configuration of the test, conducted by controlling the crack mouth opening displacement (CMOD), using a clip gauge. A servo hydraulic Instron apparatus was employed with a load cell of 100 kN capacity.

2.2 Composites analyzed

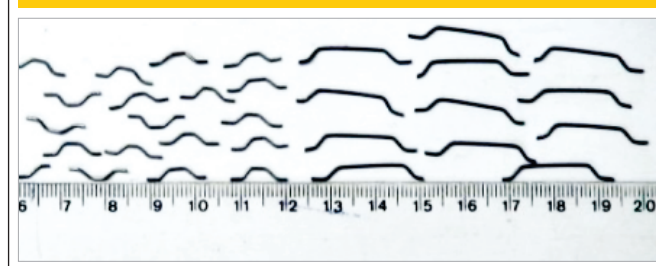
In the Stage I, thirteen composites were analyzed as shown in Table [1]. The composites were constituted by different volumes and

types of steel fiber and also different types of cement matrix (mortar and microconcrete). The obtained composites were divided into groups formed by three prisms molded with the same characteristics. In the Stage II, an additional group of six composites (all of them made of microconcrete) was analyzed.

The steel fiber specified by "A" has the commercial name *FS8-Wirand* (provided by the company *Maccaferri - América Latina*); it is 25 mm long (with hooks at its extremities) and has a diameter of 0,75 mm diameter, which results in a shape factor equal to 33. Fiber "C" was designed by Ferrari (2012) and produced by the same company specifically for this research, once this fiber is not available commercially. It is 13 mm long (with hooks at its extremities) and has a diameter of 0.75 mm, which results in a shape factor equal to 17. Because of these special characteristics, these fibers are called as steel microfibers (Fig. 4).

In the Stage II, composites containing 1,5% type A fiber were analyzed. A repetition using the composites CMP1A1C and CP-M1A2C (produced at the Stage I) was performed, but the composite CPM1A1.5C was also included. The selection of a fiber rate of 1,5% was motivated by the fact that in the Stage I this fiber rate was kept in 1%.

Figure 4 - Steel microfibers (left) and common steel fibers (right)



2.3 Composites composition and preparation

The composition of the constituting materials (Table [2]) was designed to fulfill certain practical criteria, such as:

- the use of Portland cement of high initial strength in order to obtain high strength at the first ages;
- compressive strength of 50 MPa;
- addition of superplasticizer additive to contribute to the workability of the cement paste;
- observations of the dimensional compatibility of the maximum aggregate size, which should not be greater than 1/3 of the fiber length.

The composites were produced using an electric mortar mixer with a capacity of 50 liters and an electric concrete mixer with a capacity of 300 liters. Six cylindrical specimens (100 mm x 200 mm) were molded for each composite to determine the compressive strength, the tensile strength by diametral compression and the elasticity

modulus. These specimens were kept at the same curing conditions of the prism specimens (humid chamber). Fig. 5 shows the details of the material mixtures.

In the present research, the development of composites with cement matrix constituted by mortar and microconcrete was conducted. Taking into account the fluidity of this materials when compared to concrete, they may be applied with great facility in reduced regions as the substrate of beams to be strengthened (tensile bottom chords of beams to strengthened).

It is important to note that the composites for Stages I and II were not molded at the same time. Hence, for the preparation of the composites from Stage II, the trace of the cement-based matrix from Stage I was used as initial reference, with small adjustments made according to the dosage methodology and considering the characteristics of the aggregates involved in the mixture. From Table [2], the cement consumption is observed, and the w/c ratio of the composites produced in each of the two stages are practically the same.

Table 1 - Composites analyzed

Matrix	Stage	Group	Composites	Fiber volume	Fiber type	Material	Age (days)
Mortar (A)	I	1	CPA	0%	-	mortar	29
		2	CPA1A	1%	A	mortar	29
		3	CPA1.5A	1.5%	A	mortar	29
		4	CPA2A	2%	A	mortar	29
		5	CPA1.5A0.5C	1.5%+0.5%	A+C	mortar	28
		6	CPA1.5A1.5C	1.5%+1.5%	A+C	mortar	28
		7	CPA1.5A2.5C	1.5%+2.5%	A+C	mortar	28
		8	CPA1.5A3.5C	1.5%+3.5%	A+C	mortar	28
Microconcrete (M)	I	9	CPM	0%	-	microconcrete	28
		10	CPM1A	1%	A	microconcrete	28
		11	CPM1A1C	1%+1%	A+C	microconcrete	28
		12	CPM1A2C	1%+2%	A+C	microconcrete	28
		13	CPM1A2.5C	1%+2.5%	A+C	microconcrete	28
Microconcrete (M)	II	1	CPM1A1C	1%+1%	A+C	microconcrete	50
		2	CPM1A1.5C	1%+1.5%	A+C	microconcrete	50
		3	CPM1A2C	1%+2%	A+C	microconcrete	50
		4	CPM1.5A1C	1.5%+1%	A+C	microconcrete	50
		5	CPM1.5A1.5C	1.5%+1.5%	A+C	microconcrete	50
		6	CPM1.5A2C	1.5%+2%	A+C	microconcrete	50

Nomenclature of composites

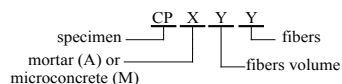


Table 2 – Composition of composite materials

Material	Mix proportion – Stage I		Mix proportion – Stage II
	Mortar	Microconcrete	Microconcrete
CP-V ARI PLUS Cement	1.0	1.0	1.00
Sand	3.0	2.13	2.30
Gravel 0	–	1.83	1.70
a/c	0.5	0.48	0.48
Cement consumption (kg/m ³)	512	446	443
Steel fiber content	variable	Variable	variable
Glenium 51	0.4%*	0.5%*	0.5%*

* The superplasticizer additive was dosed relative to the weight of the cement:

Cement density: 3.15 kg/dm³; Sand density: 2.65 kg/dm³; Gravel density: 2.87 kg/dm³; Additive density: 1.09 kg/dm³.

3. Results and discussions

3.1 Compression tests of the cylindrical specimens

The values for the mechanical properties of the composites, namely the average compressive strength (f_{cm}), the average tensile strength by diametral compression ($f_{ctm,sp}$), and the elasticity modulus (E_{cs}), are presented in Table [3] and were obtained on the same date of the flexural tests.

In general, the addition of steel fibers decreases the compressive strength of the composites for both the mortar and the microconcrete. In addition, increasing the fiber volume influenced significantly the reduction in the compressive strength. Regarding the indirect tensile strength values, a strong dispersion of the results was observed. However, for the mortar composites, an increasing in the tensile strength may be observed when increasing the volumes of type A fiber (composites 2 to 4) and microfiber (composites 5 to 8).

For the microconcrete composites produced at the Stage I, the tensile strength decreased with the increasing of the fiber volume. The exception was for the composite CPM1A2C, which presented a high value for this strength. Additionally, for the composites produced in Stage II, the highest strength value is obtained for this same composite, i.e., the composite CPM1A2C.

3.2 Loads and strengths

The flexural tenacity of the composites was determined following Rilem recommendations [6]. The criteria for tenacity evaluation is based on the energy absorption capacity, understood as the area under the force (F) versus displacement (d) curve. The contribution of these fibers to the composite tenacity is evaluated subtracting the portion of tenacity attributable to the response of the cement-based matrix.

Figure [6] illustrates a typical response of the behavior of the fiber composites under flexure, along with the expressions used for the calculation of the equivalent flexural tensile strength ($f_{eq,2}$ and $f_{eq,3}$), and the residual strengths in flexure (f_{R1} and f_{R4}). The meaning of the parameters presented in this figure are as follows:

F_L : maximum *offset* force in the interval of $\delta = 0.05$ mm. Calculated using a straight line parallel to the initial tangent, passing by the point that characterizes the displacement δ ;

δ_L : value of vertical displacement corresponding to F_L ;

$f_{fct,L}$: stress corresponding to F_L , given by:

$$f_{fct,L} = \frac{3 \cdot F_L \cdot L}{2 \cdot b \cdot h_{sp}} \quad (1)$$

L : specimen clearance;

b : specimen width;

h_{sp} : distance from the top of the notch top to the top face of the specimen;

$D_{BZ,2}^b$, $D_{BZ,2}^f$, and $D_{BZ,3}^f$: energy absorption capacity of the matrix and the fibers, respectively. Calculated by the area under the F - δ curve until specific displacements, as shown in Figure 6;

$F_{R,1}$ and $F_{R,4}$: forces corresponding to the displacements $\delta_{R,1} = 0.46$ mm and $\delta_{R,4} = 3.0$ mm. These values are used to calculate the residual flexural tensile strengths.

The tenacity parcels $D_{BZ,2}^f$ and $D_{BZ,3}^f$ are transformed into equivalent flexural tensile strength for the two different displacement levels d_2 and d_3 , respectively, as indicated by Figure 6. The material load capacity relative to the pre-defined maximum displacement value is evaluated using the concept of residual flexural strength ($F_{R,1}$ and $F_{R,4}$).

Table [4] presents the strength and load values calculated based on Rilem recommendations [6]. The value of the maximum load of composite is also presented (F_M).

Figure 5 – Detail of the appearance of the material mixture



Table 3 – Average results of composite characterization under compression

Matrix	Stage	Groups	Composites	f_{cm} (MPa)	$f_{cm,sp}$ (MPa)	E_{cs} (GPa)
Mortar (A)	I	1	CPA	52.5	3.1	23.8
		2	CPA1A	43.8	3.7	22.7
		3	CPA1.5A	42.2	3.7	23.1
		4	CPA2A	45.7	4.9	24.0
		5	CPA1.5A0.5C	49.2	4.4	28.2
		6	CPA1.5A1.5C	47.2	4.9	32.3
		7	CPA1.5A2.5C	43.6	4.8	31.0
		8	CPA1.5A3.5C	42.8	4.9	29.1
Matrix	Stage	Groups	Composites	f_{cm} (MPa)	$f_{cm,sp}$ (MPa)	E_{cs} (GPa)
Microconcrete (M)	I	9	CPM	62.3	3.8	35.2
		10	CPM1A	42.0	3.0	30.6
		11	CPM1A1C	40.6	3.7	26.3
		12	CPM1A2C	42.8	5.1	30.0
		13	CPM1A2.5C	20.8	2.8	19.9
Matrix	Stage	Groups	Composites	f_{cm} (MPa)	$f_{cm,sp}$ (MPa)	E_{cs} (GPa)
Microconcrete (M)	II	1	CPM1A1C	33.2	2.5	32.3
		2	CPM1A1.5C	30.6	2.2	31.0
		3	CPM1A2C	33.4	3.2	32.4
		4	CPM1.5A1C	28.3	2.6	29.8
		5	CPM1.5A1.5C	30.5	2.9	31.0
		6	CPM1.5A2C	29.2	2.4	30.2

For each composite, three specimens were subjected to axial compression test and three to the diametral compression tensile test.

E_{cs} – secant deformation modulus corresponding to the inclination of the secant line in the stress-strain diagram, passing by the points corresponding to the 0.5 MPa stress and 30% of the compressive strength.

The value of the parameter $f_{fct,L}$ represents the portion of the composite strength due to the cement-based matrix. The addition of steel fibers visibly contributed to the increasing of this

strength (Figure [7]). It can also be stated that the addition of microfibers to the steel fibers improved even more the composite strength for the mortar composites. Once the values of

Figure 6 – Rilem criteria for the evaluation of the behavior of fibrous material

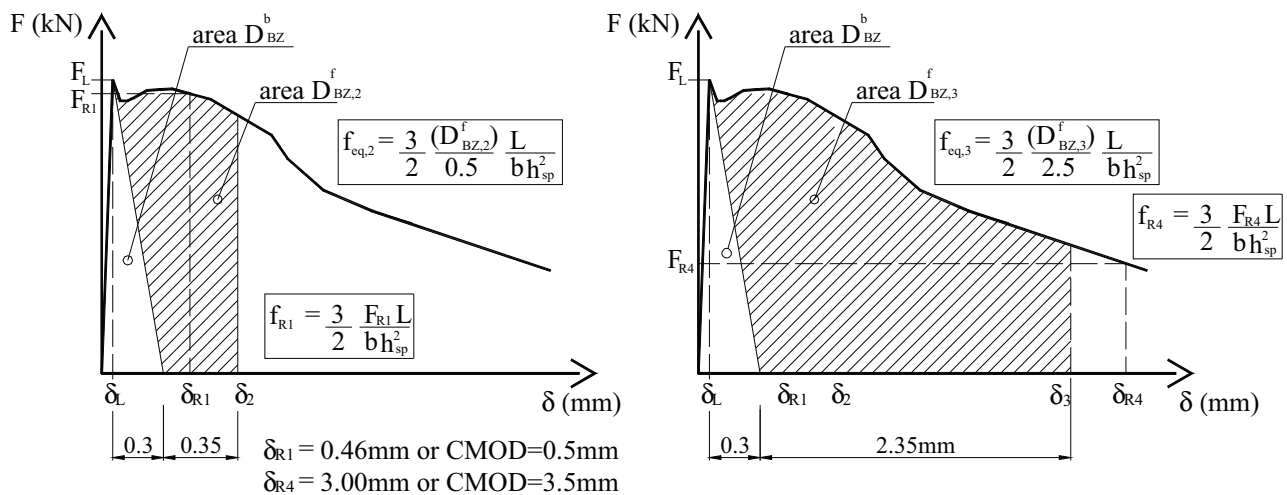
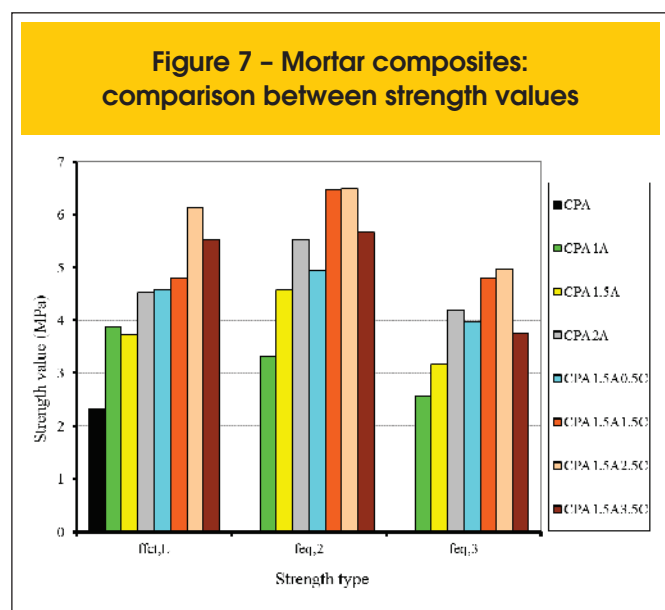


Table 4 – Load and strength according to RILEM

Matrix	Stage	Composites	Loads (kN)				Loads (kN)				
			F_L	F_M	$F_{R,1}$	$F_{R,4}$	$f_{fct,L}$	$f_{eq,2}$	$f_{eq,3}$	$f_{R,1}$	$f_{R,4}$
Mortar (M)	I	CPA	8.0	8.0	1.3	–	2.3	–	–	0.4	–
		CPA1A	13.4	13.4	12.5	5.2	3.9	3.3	2.6	3.6	1.5
		CPA1.5A	13.1	16.1	16.0	6.1	3.7	4.6	3.2	4.5	1.7
		CPA2A	14.5	17.6	17.4	7.6	4.6	5.5	4.2	5.5	2.4
		CPA1.5A0.5C	16.4	17.8	17.2	9.3	4.6	4.9	4.0	4.8	2.6
		CPA1.5A1.5C	16.0	21.0	20.9	9.4	4.8	6.5	4.8	6.3	2.8
		CPA1.5A2.5C	22.1	23.7	23.5	12.8	6.1	6.5	5.0	6.5	3.6
		CPA1.5A3.5C	20.0	21.4	20.8	6.1	5.5	5.7	3.8	5.7	1.7
Microconcrete (M)	I	CPM	14.1	14.2	1.3	–	4.0	–	–	0.4	–
		CPM1A	12.0	12.1	7.5	3.7	3.3	2.0	1.6	2.1	1.0
		CPM1A1C	17.6	18.5	16.9	7.5	5.2	5.1	3.7	5.0	2.2
		CPM1A2C	19.4	21.9	19.7	8.0	5.5	5.7	4.1	5.7	2.3
		CPM1A2.5C	10.0	10.0	6.3	2.3	2.9	1.5	1.1	1.9	0.7
		Microconcrete (M)	II	CPM1A1C	12.2	14.3	11.4	1.0	3.6	3.5	2.4
CPM1A1.5C	12.0			15.2	12.1	2.7	3.5	3.8	2.5	3.6	0.8
CPM1A2C	14.4			18.9	15.9	1.8	4.1	4.9	3.0	4.5	0.5
CPM1.5A1C	12.8			18.5	16.0	2.4	3.7	5.0	2.4	4.6	0.7
CPM1.5A1.5C	15.2			19.8	17.5	1.3	4.3	5.3	3.6	5.0	0.4
CPM1.5A2C	11.0			15.6	13.4	3.2	3.2	4.4	2.9	4.0	1.0

equivalent flexural strength ($f_{eq,2}$ and $f_{eq,3}$) represent the behavior of the composites based on the contribution of the fibers, Figure [7] also suggests an increasing in the flexural strength due to



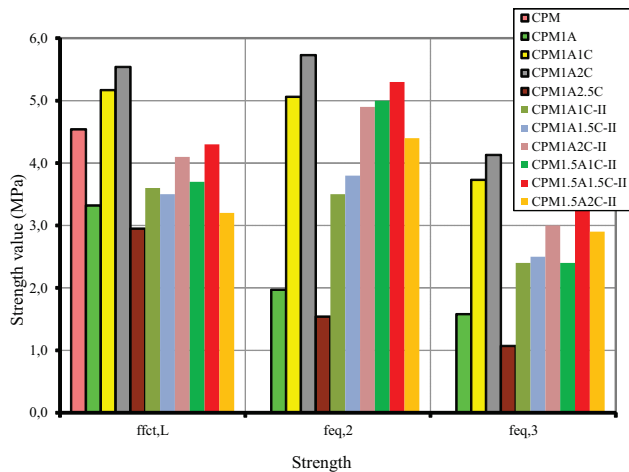
the increasing of fiber A volume, especially when steel microfibers are added.

The strength values for the microconcrete composites are compared in Figure [8]. It is important to note the drop in the strength $f_{fct,L}$ of the composite CPM1A in comparison to the composite CPM, which demonstrates that the isolated presence of steel fiber A did not improve the strength of the cement-based matrix. By incorporating steel microfiber (C) with fiber (A), the contribution of fibers to the flexural strength is significantly increased for the composites CPM1A1C and CPM1A2C.

Regarding the flexural strength values, the increase of such strengths by the addition of steel microfiber to fiber A is notable. In the majority of composites, the equivalent strength $f_{eq,2}$ surpasses the value of the strength $f_{fct,L}$. This result indicates significant strength gains even after the cracking. Particular attention is drawn to the behavior of the composites CPM1A2C and CPM1.5A1.5C-II, with the latter produced in the Stage II. It should be mentioned that composite CPM1.5A1.5C-II was produced intending to complement the amount of fibers investigated in the Stage I.

Regarding the values of equivalent flexural strength ($f_{eq,3}$), which represents the graph area until the vertical displacement (d_3), the higher tenacity of the previously cited composites can be highlighted, as well as the high tenacity of composite CPM1A1C.

Figure 8 - Microconcrete composites: comparison between the strength results



3.3 P-CMOD curves

The P-CMOD curves of mortar composites are presented in Figure [9]. The presence of steel fibers and steel microfibers in the cement-based mortar matrix increased the energy absorption capacity and the strength levels before and after the matrix cracking. Increasing the type A fiber volume delivered some improvement in the composites ductility. With the addition of 0,5% of steel microfibers, however, it was possible to elevate the energy absorption capacity of the composite CPA1.5A to the same level as CPA2A. This elevation is advantageous taking into account that the workability of the composite is not modified by the microfiber. By another

hand, the workability of the composite is significantly influenced by the increasing of the type A fiber.

The maximum values of force (F_M), obtained for composites CPA1.5A0.5C and CPA2A, are practically the same, i.e., 17,78 kN and 17,59 kN, respectively. The same behavior may be also observed for the flexural strength ($f_{ct,L}$), with values of 4,58 MPa and 4,56 MPa, respectively. The same statement may be established to the residual strength ($f_{R,1}$ e $f_{R,4}$) for this two mentioned composites.

To visualize the effect of the steel microfibers in the initial Stage of the composite performance, Figure [10] shows the same curves displayed by Figure [9], but now emphasizing the initial composite loading interval (CMOD up to 0.15 mm). In the composites with fiber A isolated, the branch after the matrix cracking is well defined with constant strength and variable CMOD. However, in the presence of microfibers, the stress transfer is gradual and occurs with increasing strength of the composites. The stress transfer process with cracking of the matrix is facilitated by the presence of microfibers. The dispersion of microfibers in the matrix increases the possibility of interception of cracks, sewing the cracks and increasing the composite strength.

All P-CMOD curves of microconcrete composites are shown in Figure [11]. The presence of fibers and microfibers particularly improved the energy absorption capacity of these composites. The strength capacity was decreased with the isolated presence of fiber A (composite CPM1A). However, with the incorporation of 1% of type A steel fibers and 2% of microfibers, higher strength and energy absorption levels were reached. The same phenomenon was not verified for the incorporation of 2.5% microfibers.

The maximum force reached by the composite CPM1A2C was 37% and 61% above the forces obtained for the composites CPM and CPM1A, respectively. By another hand, the equivalent flexural strength ($f_{eq,2}$) of the composite CPM1A2C was 110% and 13% above the strength obtained for the composites CPM1A and CPM1A1C, respectively.

Figure 9 - P-CMOD curves of the mortar composites

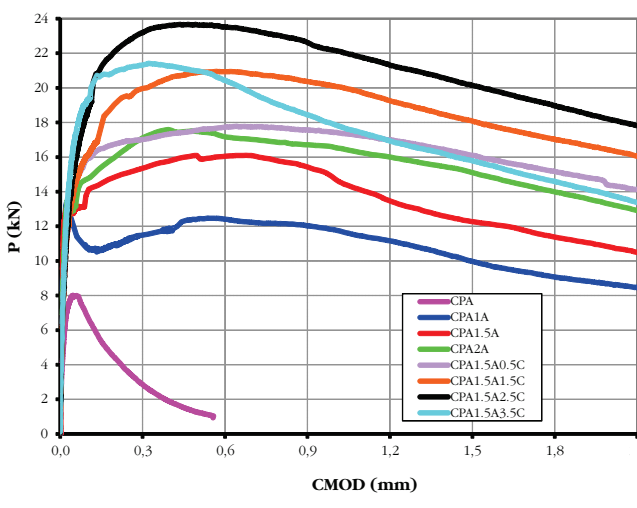


Figure 10 - Initial P-CMOD behavior of the mortar composites

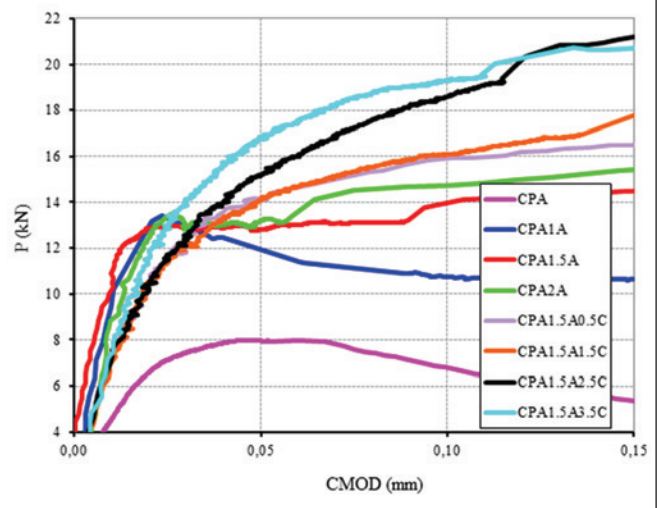


Figure 11 - P-CMOD curves of the microconcrete composites

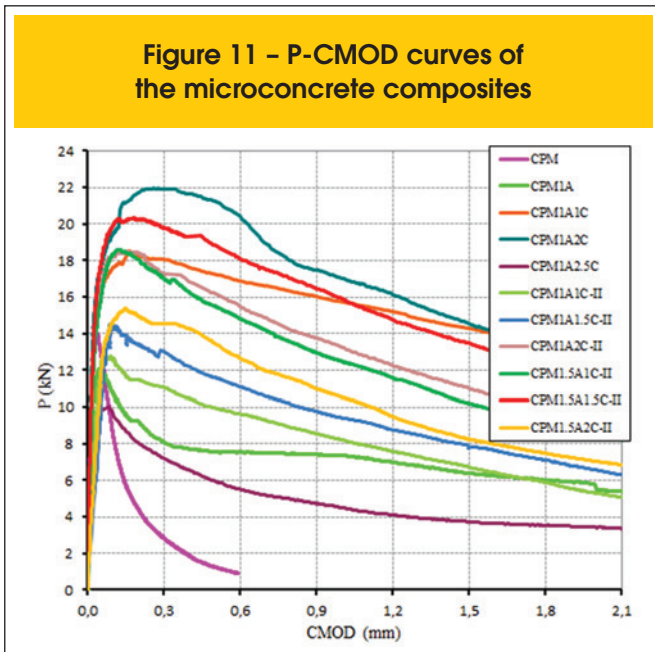
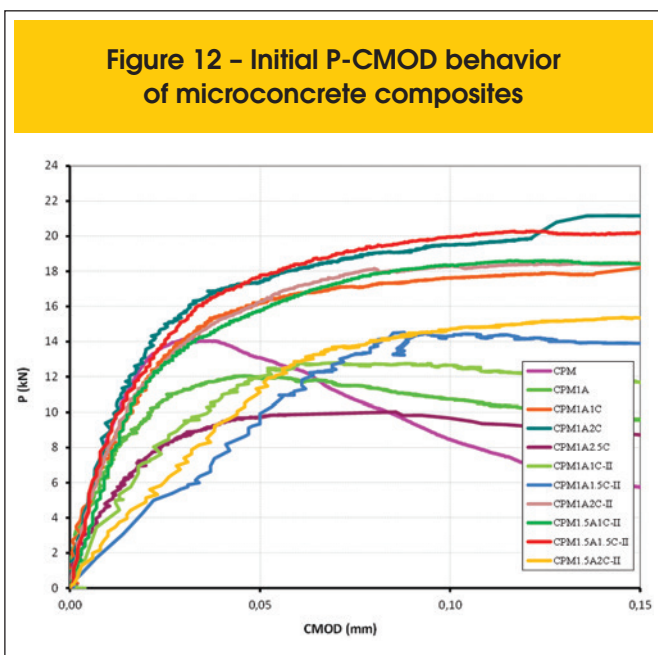


Figure [12] visualizes the effect of microfibers on the stress transfer process in the microconcrete matrix. Note that, as the matrix cracks, the matrix-fiber stress transfer process occurs with the elevation of strength levels in the composites CPM1A1C and CPM1A2C due to the presence of microfibers.

With the matrix cracking, based on the presence of microfibers, it was observed that the matrix-fiber stress transfer process occurred with increasing strength levels for the composites CPM1A1C, CPM1A2C, CPM1A2C-II, CPM1.5A1C-II and CPM1.5A1.5C-II. Furthermore, an improvement on the behavior of these materials was observed when microfiber volume increases from 1% to 2%, and from 1% to 1,5% for the composites produced in Stages I and II, respectively.

Figure 12 - Initial P-CMOD behavior of microconcrete composites



3.4 Fracture strength curves

Figure [13] presents the fracture strength curves of each cement-based mortar composites. Figures [14] and [15] present the fracture strength curves of microconcrete composites produced in Stages I and II, respectively. In these figures, “ K_R ” indicates the fracture strength of the composite, and parameter “ a ” is the depth of the crack (a) standardized by the height (W) of the prism specimen, i.e., $a = a/W$.

For the prism specimens (see Figure [3]) the values of K_R were obtained from the P-CMOD values using equation [2], which is only valid for fracture Mode I. In this equation, the parameters are as described in Figure [3], where function $f(a)$ depends on the geometry and is determined using the procedures described by Ferreira [4].

$$K_R = \frac{1.5PS\sqrt{\pi a}}{BW^2} f(\alpha) \tag{2}$$

From the analysis of the strength curves, it is possible to extract information about the performance of the composites in terms of strength to crack propagation. The final branches of the strength curves of the composites are rising, representing the post-peak phase of the loading history, where the gain of strength to crack propagation given by the steel fibers and microfibers is high.

From Figure [13], regarding the matrix without fibers (CPA), the expected low strength capacity to crack propagation is observed, evidenced by the small extension of the initial vertical branch. This fact suggests the subcritical spread of cracks even at low loading levels, eventually caused by the absence of coarse aggregates in the mixture. Nevertheless, the presence of fibers and microfibers in the matrix slowed this phenomenon.

Even for small propagations of cracks ($a = 0,2$), the fracture strength of the composites with fibers were higher (between 33% to 18% depending on the volume of fibers) than the composites without fibers (CPA). The higher and the lower strengths to the

Figure 13 - Strength curves for the mortar composites

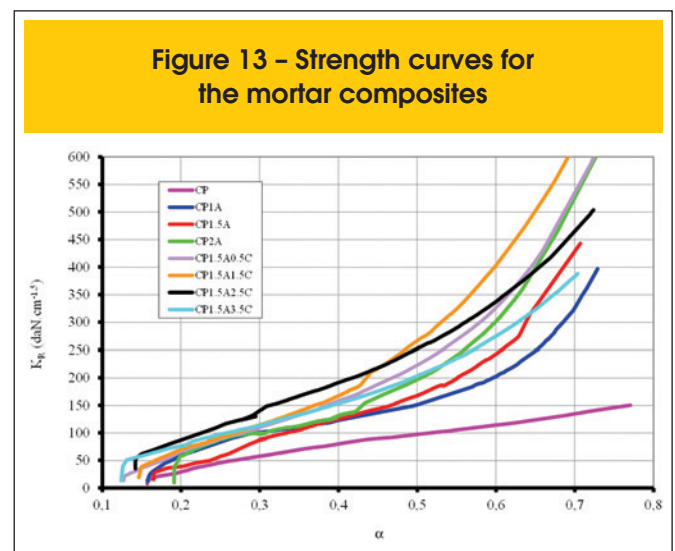
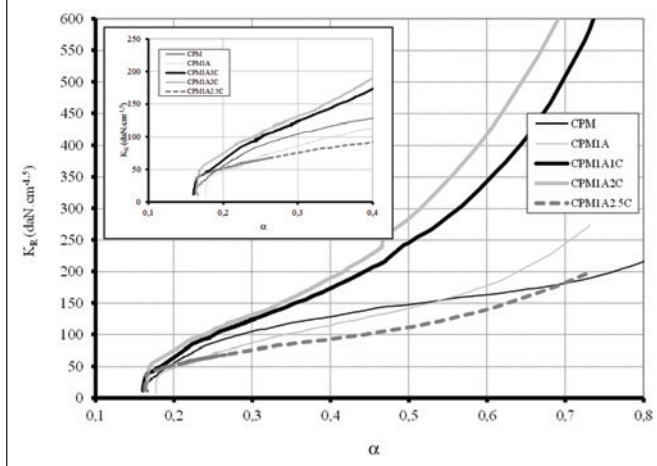


Figure 14 – Strength curves for microconcrete composites – Stage I



propagation of cracks were obtained for composites CPA1.5A2.5C and CPA1.5A, respectively. From Figure [13], is possible to observe that the higher gains of strength were obtained adding the type C microfibers to the type A fibers.

The fracture strength gain was well evidenced, especially in the post-peak branch. Among the mortar composites, the greatest fracture strength gain were observed for the composites CPA1.5A1.5C and CPA1.5A2.5C.

From Figure [14], it can be observed that for small crack propagation, the fracture strength of the composites CPM1A and CPM1A2.5C are lower than that one for composites without fibers. However, for more advanced stages of crack propagation, a > 0.6, the fracture strength of these composites surpass the fracture strength of the matrix without fibers. For the latter, the curve configuration (small declivity compared to the others) indicates low strength of the material to the crack propagation.

For a = 0.2, the fracture strengths of composites CPM1A1C and CPM1A2C were, respectively, 18% and 36% higher than the matrix without fibers. Compared to composite CPM1A, the increases were even more significant, 44% and 66%, respectively, demonstrating the beneficial effects of the microfibers on the fracture strength.

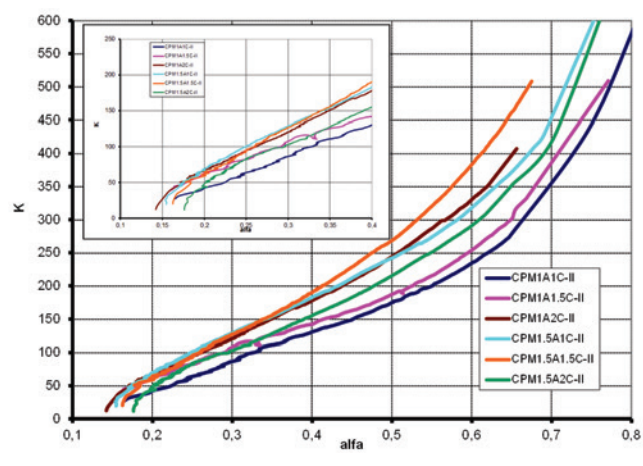
From Figure [15], it is evident that the fracture strength performance of the composites containing 1% of fibers improved gradually with increasing steel microfiber content. The same behavior is observed only for composites CPM1.5A1C-II and CPM1.5A1.5C-II containing 1.5% of steel fibers. Additionally, the performance of composite CPM1.5A2C-II was inferior to the others of its series.

4. Conclusions

From the conducted research, the following observations may be established:

- The hybridization process is an interesting alternative for application in the recovery of tensile bottom chord of beams, once the addition of microfibers to the steel fibers increased the tensile stress in flexure and increased the flexural tenacity of the cement-based mortar and microconcrete composites;

Figure 15 – Strength curves for microconcrete composites – Stage II



- With the cracking of the cement-based matrix, the stress transfer was facilitated by the steel microfibers, which being dispersed in the matrix in higher amounts, conditioned the crack propagation to the increase of the loading level;
- Considering the pseudo-hardening characteristic and its specific application, composite CPM1A2C presented the greatest qualities among the products of the Stage I, designed for application to the reconstruction of the tensile bottom chords of reinforced concrete beams strengthened in flexure with CFRP sheets;
- Among the composites produced in the Stage II, the behavior of CPM1.5A1.5C-II was noteworthy, as the hybridization process provided considerable increases in the maximum load as well as in the flexural and fracture strengths.

5. Acknowledgements

We thank FAPESP, CAPES and CNPq for financial support. We also thank Maccaferri-Latin America for the production, under contract, of the steel microfibers.

6. References

- [01] Bentur, A., Mindess, S. (1995). Fiber Reinforced Cementitious Composites, Elsevier, London, 1990.
- [02] Yao, W., Li, J., Wu, K. (2003). Mechanical properties of hybrid fiber-reinforced concrete at low fiber volume fraction. Cement and Concrete Research, 33, 27-30.
- [03] Mobasher, B., Li, C.Y. (1996). Mechanical properties of hybrid cement-based composites. ACI Mater. J. 93 (3), 284-292.
- [04] Ferreira, L.E.T.; Bittencourt, T.N.; Souza, J.L.A.O.; Gettu, R. (2012). R-Curve behavior in notched beam tests of rocks. Engineering Fracture Mechanics, N. 32, 27-40.
- [05] Ferrari, V. J.; Hanai, J.B. (2012). "Flexural strengthening of reinforced concrete beams with carbon fibers reinforced polymer (CFRP) sheet bonded to a transition layer of high performance cement-based composite". Ibracon Structures and Materials Journal, v. 5, n. 5, 596-626.

- [06] Rilem TC 162-TDF (2002). "Test and design methods for steel fibre reinforced concrete. Bending test" *Materials and Structures*, v. 35, 579-582.
- [07] Arquez, A. P. Aplicação de laminado de polímero reforçado com fibras de carbono (PRFC) inserido em substrato de microconcreto com fibras de aço para reforço à flexão de vigas de concreto armado. Dissertação – Escola de Engenharia de São Carlos da Universidade de São Paulo, 2010.